KeAi

CHINESE ROOTS
GLOBAL IMPACT

Contents lists available at ScienceDirect

Petroleum Science

journal homepage: www.keaipublishing.com/en/journals/petroleum-science



Original Paper

Logging identification method of depositional facies in Sinian Dengying Formation of the Sichuan Basin



Qing-Fu Feng ^{a, *}, Yu-Xiang Xiao ^a, Xiu-Lin Hou ^a, Hong-Kui Chen ^b, Ze-Cheng Wang ^a, Zhou Feng ^a, Han Tian ^a, Hua Jiang ^a

- ^a Research Institute of Petroleum Exploration & Development, Beijing, 100083, China
- ^b College of Geosciences, China University of Petroluem (Beijing), Beijing 102249, China

ARTICLE INFO

Article history: Received 23 July 2020 Accepted 28 October 2020 Available online 12 July 2021

Edited by Jie Hao

Keywords:
Deng 4 member
Core calibration
Microfacies
Electrical image log
Log facies
Karst reservoir

ABSTRACT

The sedimentary facies/microfacies, which can be correlated with well logs, determine reservoir quality and hydrocarbon productivity in carbonate rocks. The identification and evaluation of sedimentary facies/microfacies using well logs are very important in order to effectively guide the exploration and development of oil and gas. Previous carbonate facies/microfacies identification methods based on conventional well log data often exist multiple solutions. This paper presents a new method of facies/ microfacies identification based on core-conventional logs-electrical image log-geological model, and the method is applied in the fourth member of the Dengying Formation (Deng 4) in the Gaoshiti-Moxi area of the Sichuan Basin, Firstly, core data are used to calibrate different types of facies/microfacies, with the aim to systematically clarify the conventional and electrical image log responses for each type of facies/microfacies. Secondly, through the pair wise correlation analysis of conventional logs, GR, RT and CNL, are selected as sensitive curves to establish the microfacies discrimination criteria separately. Thirdly, five well logging response models and identification charts of facies/microfacies are established based on electrical image log. The sedimentary microfacies of 60 exploratory wells was analyzed individually through this method, and the microfacies maps of 4 layers of the Deng 4 Member were compiled, and the plane distribution of microfacies in the Gaoshiti-Moxi area of the Sichuan Basin was depicted. The comparative analysis of oil testing or production results of wells reveals three most favorable types of microfacies and they include algal psammitic shoal, algal agglutinate mound, and algal stromatolite mound, which provide a reliable technical support to the exploration, development and well deployment in the study area.

© 2021 The Authors. Publishing services by Elsevier B.V. on behalf of KeAi Communications Co. Ltd. This is an open access article under the CC BY-NC-ND license (http://creativecommons.org/licenses/by-nc-nd/

4.0/).

1. Introduction

Carbonate rock reservoirs generally have complex and heterogeneous pore networks due to various porosity enhancing, preserving or destroying modifications or activities (Westphal et al., 2005; Hollis et al., 2010; Roth et al., 2011; Norbisrath et al., 2015; Lai et al., 2020). Prediction of reservoir quality via petrophysical logs becomes difficult (Lai et al., 2019; Wang et al., 2020). However, reservoir quality in carbonate rocks is primarily controlled by depositional facies, and these facies-controlled carbonate rocks can

E-mail address: fengqingfu@petrochina.com.cn (Q.-F. Feng).

be predicted via well logs if the depositional facies can be evaluated and predicted.

The Sinian Dengying Formation in the Sichuan Basin is one of the important strata for gas exploration, and contains mound/shoal facies reservoirs altered by karstification. The Gaoshiti-Moxi area is located in the eastern slope of the Caledonian paleo-uplift, with the original gas in place (OGIC) exceeding one trillion cubic meters in the Dengying Formation (Li et al. 2013a; Zou et al., 2014; Wei et al., 2015). So far, the exploration of the Deng 4 Member (Member 4 of Dengying Formation) has shifted from the platform margin to the intra-platform where the reservoir quality is quite different. For facies-controlled reservoirs (reservoir quality is determined by depositional facies), the identification and plane distribution of microfacies are critical for the exploration and development (Yao et al., 2014; Luo et al. 2015, 2019; Shan et al., 2016; Song et al.,

 $^{^{*}}$ Corresponding author. Research Institute of Petroleum Exploration & Development, Beijing, 100083, China.

Q.-F. Feng, Y.-X. Xiao, X.-L. Hou et al. Petroleum Science 18 (2021) 1086-1096

2017; Lan et al., 2019; Lai et al., 2019). However, it is difficult to characterize the succession of microfacies in the vertical direction and the types of microfacies in the horizontal direction, which restricts the further exploration and development in the study area.

To characterize the vertical and horizontal distribution of depositional facies are difficult due to limited core data, therefore well log data are needed to predict depositional facies (Li et al., 2014). A lot of works have been conducted on identifying sedimentary microfacies with conventional log methods (Mancini et al. 2000, 2008; Lai et al., 2019). However, conventional log methods can only identify limited types of sedimentary microfacies from the prospective of mineral composition or response characteristics, generating multiple solutions. In contrast, electrical image log can provide high-resolution images to clearly reveal the texture and structure characteristics (Lai et al., 2020). Nevertheless, it is still challenging to accurately establish the image log identification chart for microfacies and minimize the ambiguity of resolutions.

The Dengying Formation in the Sichuan Basin is mainly composed of deposits of carbonate platform margin and restricted platform facies. In previous studies, core and thin section data were used to calibrate conventional logs, and mathematical statistical methods were adopted to establish well log microfacies patterns and identify the conventional log responses of various types of sedimentary microfacies; however, this method is defective for low resolution and multiple solutions. Alternatively, outcrop can be combined with a small amount of core and thin section data to calibrate the seismic data, with the aim to characterize the sedimentary facies in space; however, this method cannot accurately recognize the microfacies, but only reach the subfacies scale with low accuracy (Riding, 1991; Riding, 2000). The combination of conventional log and image log has been rarely studied for characterizing the facies/microfacies in the study area. Image logs measures the two-dimensional or three-dimensional distribution of resistivity or wave impedance of rocks along the borehole wall or around the borehole by way of scanning and array, and forms the digital image of the well profile to indirectly show the geological features such as fracture, suture, bedding, cavities, muddy filling, and siliceous agglomerates; this method is intuitive and has high resolution (Yang et al., 2014; Lai et al., 2018).

In this paper, based on previous studies, together with the results of core description and thin section identification for 20 coring wells, the electrical image log models of 8 types of microfacies in the Deng 4 Member through core-calibration logging, and the logging identification chart and corresponding geological model and lithological model are established for each type of microfacies. The research results provide a reliable technical support to identification of depositional microfacies, and will provide guidance for the exploration and development of carbonate rocks in Sichuan Basin.

2. Samples and methods

More than 100 wells are drilled in the Gaoshiti-Moxi area. Cores are taken from 20 wells. Detailed core descriptions focused on the lithology, sedimentary structure, bedding characteristics and depositional facies analysis (Lai et al., 2017).

The conventional log suits include caliper (CAL), natural gamma ray (GR), compensated neutron porosity (CNL), bulk density (DEN), sonic interval transit time (AC), resistivity (Rt, Rxo). Borehole electrical image logs are classified as unconventional well logs, are collected in more than 20 cored wells, therefore the calibration between cores and image logs for structural and sedimentary characteristics is possible. The image logs are collected in water-based drilling muds using a Halliburton's EMI/XRMI (Extended Range Microlmager) tool. The borehole coverage is approximately

60% in an 8.5 inch hole, and have a vertical resolution down to 5 mm (Awdal et al., 2016; Lai et al. 2017, 2018). The image log raw data (i.e. nti files) were processed using the Schlumberger's Techlog software through the process such as speed correction, eccentering correction, and normalization (Xu et al., 2009; Khoshbakht et al. 2009, 2012, 2012; Lai et al., 2018). Then the processed high resolution images can be used for sedimentary interpretation (Goodall et al., 1998; Folkestad et al., 2012; Keeton et al., 2015; Brekke et al., 2017).

The shifting of core depth to image log depth was achieved by correlating core-based density with bulk density curve (DEN) to identify distinctive features and match the depths.

The natural gamma log, resistivity log and neutron log that are sensitive to sedimentary microfacies are selected to make well log crossplot of microfacies, by which the conventional logging responses of different microfacies are summarized. Coupling with the electrical image logs, which is characterized by high resolution and full-borehole coverage, a new log identification method of sedimentary microfacies and relevant process are formed (Geng et al., 2002; Yang et al., 2014; Wang et al., 2016; Zhou et al., 2017) (Fig. 1). Fundamentally, the logging facies model should be transformed into geological microfacies pattern, therefore the vertical succession and plane distribution of sedimentary facies can be accurately described. Therefore, the high quality reservoirs can be predicted using well logs according to the relationship between high-quality reservoir and sedimentary facies, thereby providing technical support for the exploration, development and geological research.

3. Sedimentary facies in the Dengying Formation

Previous studies of lithofacies paleogeography for gas exploration in the Dengying Formation in the Sichuan Basin revealed evaporative tidal flat and evaporative lagoon facies in all areas, except for grain shoal facies in the Ziyang-Weiyuan structure, but failed to uncover any high-energy facies belt (Hu et al., 2019; Wang et al., 2019). Since 2011, great efforts have been made to analyze the drilling, logging and testing data, investigate the seismic and outcrop sections and map the lithofacies paleogeography integrating both structure and deposits. As a result, an intra-cratonic platform margin high-energy facies belt was discovered. This belt distributes in a "U" shape, symmetrically on the sides along the N-S-trending Deyang-Anyue intra-cratonic rift. This discovery changed the traditional understanding that the Sinian structure in the Upper Yangtze craton is structurally stable and simple in sedimentary facies (Song et al., 2013; Liu et al., 2016; Wen et al., 2017; Zhang et al., 2019).

It is generally believed that, in the depositional period of the Dengying Formation, the Sichuan Basin was covered in shallow and restricted sedimentary waters, which became open eastward. The sedimentary facies can be divided into platform flat, tidal flat, ramp, and platform. The Dengying Formation in the Upper Yangtze area exhibits the alternate deposits of ramp and tidal flat. Within the basin, shallow, relatively occluded, restricted platform facies is dominant, which can be subdivided into three subfacies: lagoon, tidal flat, and intra-platform shoal (Wu et al., 2013; Yang et al., 2014; Duan et al., 2019). The Deng 4 Member in the Gaoshiti-Moxi area is divided into 7 types of subfacies and 12 types of microfacies (Table 1). The microfacies can be easily identified through well logs combined with the core and thin sections. Then, a new model of microfacies association (consisting of 12 microfacies) in the Deng 4 Member in the Gaoshiti-Moxi area is established (Fig. 2).

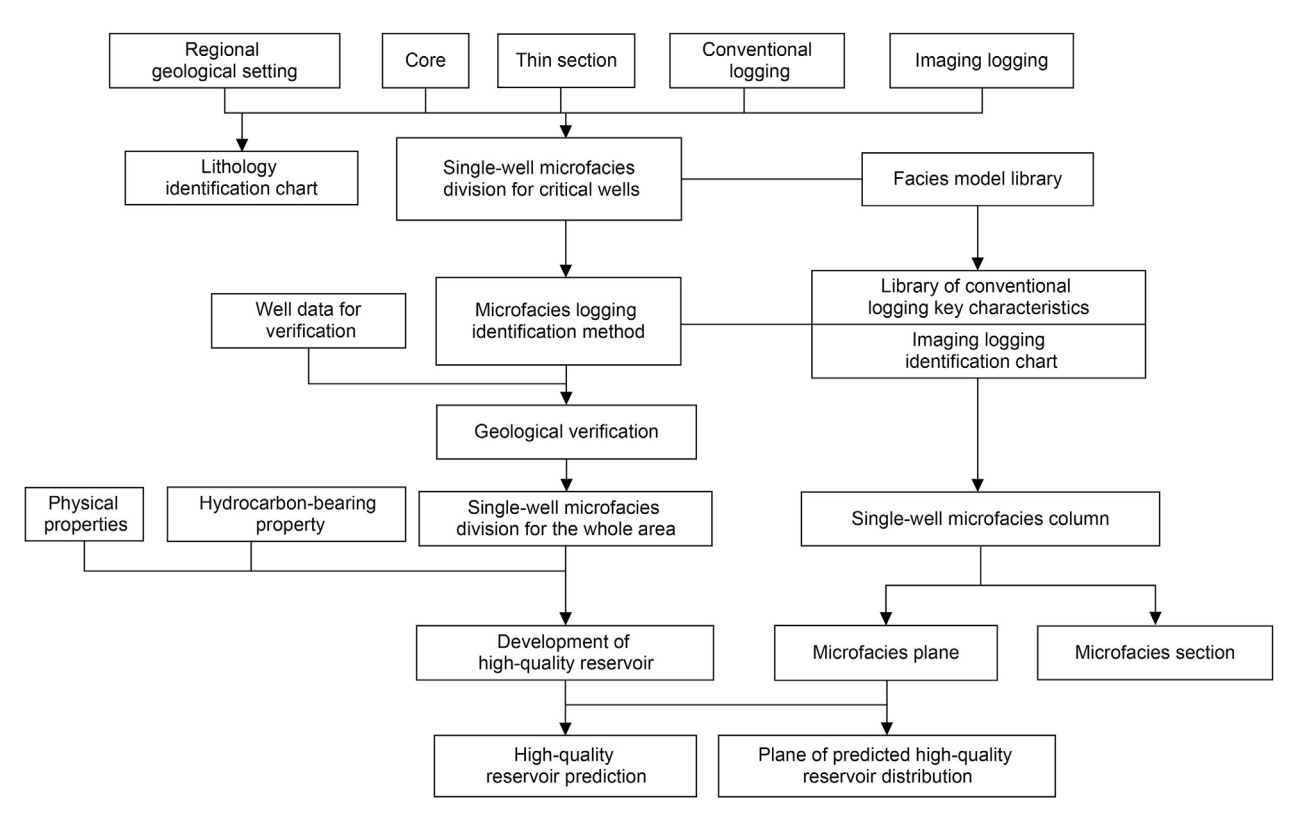


Fig. 1. Roadmap of logging identification method of sedimentary microfacies.

Table 1 Sedimentary facies in the Gaoshiti-Moxi area, the Sichuan Basin.

Facies	Subfacies	Microfacies	Lithologies	
Platform margin	Platform margin grain shoal	Algal psammitic shoal	Light grey—brownish grey granular dolomite	
	Platform margin algal mound	Algal laminae mound	Siliceous algal laminae dolomite	
		Algal agglutinate mound	Algal agglutinate dolomite	
		Algal stromatolite mound	Algal stromatolite dolomite	
	Inter-shoal sea	Dolomitic inter-shoal sea	Greyish black dolomicrite	
Restricted platform	Intra-platform grain shoal	Algal psammitic shoal	Light grey-brownish grey algalpsammitic dolomite	
	Intra-platform algal mound	Algal laminae mound	Algal laminae dolomite	
		Algal agglutinate mound	Algal agglutinate dolomite	
	Platform flat	Algal dolomite flat	Grey-brownish greysilty-fine crystal algal dolomite	
		Dolomite flat	Grey-brownish greysilty-fine crystal dolomite	
		Argillaceous dolomite flat	Grey-brownish grey argillaceous dolomicrite	
	Inter-shoal sea	Dolomitic inter-shoal sea	Greyish blackdolomicrite	

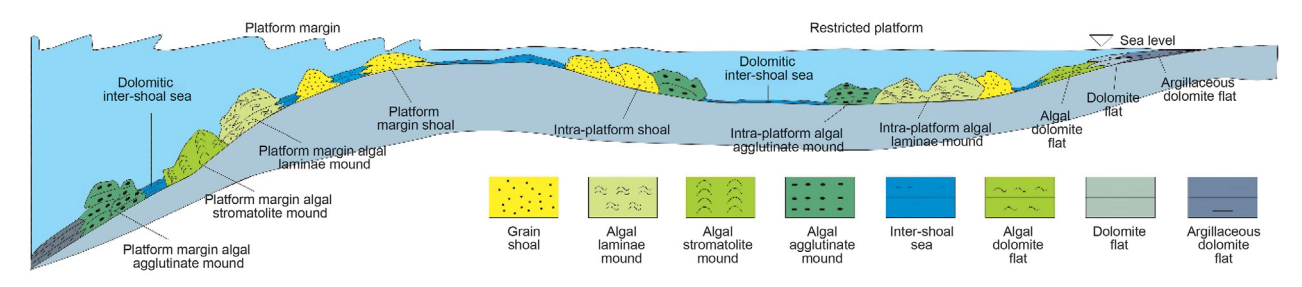


Fig. 2. Model of microfacies association of the Deng4 Member in the Gaoshiti-Moxi area (Li et al., 2013b)

4. Results

4.1. Microfacies identification by conventional logs

Conventional log is used to identify sedimentary microfacies of

carbonate rocks through: (1) determining critical wells in oil and gas fields; (2) building the geological microfacies pattern for carbonate rocks; (3) clarifying the geological depositional and logging response characteristics; (4) correcting and normalizing the log data depending on setting; (5) analyzing the correlation between

Q.-F. Feng, Y.-X. Xiao, X.-L. Hou et al. Petroleum Science 18 (2021) 1086-1096

log data and geological microfacies; (6) adopting various mathematical statistical methods to establish logging microfacies pattern; and (7) verifying the division of logging microfacies and modifying the model. The mathematical methods mentioned include fuzzy identification system, stepwise regression method, fuzzy expert system, Bayes stepwise discrimination method, grey correlation analysis method, and the likes.

In this study, a total of 520 m core samples from 20 wells were selected. Three conventional logs, i.e. GR (natural gamma log), CNL (neutron log) and RT (deep lateral resistivity), which are sensitive to sedimentary facies, were selected to prepare the GR-RT, GR-CNL and RT-CNL crossplots for platform margin and intra-platform. The GR-RT and GR-CNL crossplots of platform margin microfacies (Fig. 3a and b) show that the CNL-GR crossplot can distinguish the microfacies of algal laminae mound, inter-shoal sea and moundshoal complex. Specifically, the inter-shoal sea has relatively high GR value (>20 API) and also high CNL value, while the algal laminae mound has relatively low GR and CNL values. The algal psammitic shoal and the algal agglutinate mound cannot be distinguished, since their data points overlap; thus, they are collectively referred to as the mound-shoal complex. Based on these crossplots, the conventional logging identification criteria for carbonate microfacies of the Deng 4 Member in the Gaoshiti-Moxi area were preliminarily established (Table 2). Merely, this method is defective for strong ambiguity and low accuracy.

4.2. Model of image log microfacies

According to the presence of geological information in image logs, image log can be divided into two models: geological model and non-geological model. The geological model can be divided into the types of tight layer, loosen layer, interlayer, bedding surface, erosion surface, unconformity, bedding, fracture, fault, cavity, gravel and symmetrical furrow. The non-geological model can be divided into the types of twill, wood grain, asymmetric furrow and blank. In this study, the cores of the Deng 4 Member were restored to deeply match the conventional logs, core and image logs. The cores were used to calibrate image log and the test data were comprehensively analyzed. Totally, 60 typical core-image log response charts were prepared for the image log facies of the Deng 4 Member. The imaging characteristics of the Deng 4 Member were categorized into five facies patterns: (1) porphyritic, (2) massive, (3) layered, (4) linear, and (5) strip (Fig. 4), which were subdivided into nine microfacies patterns. Specifically, the porphyritic facies pattern is subdivided into chaotic dark porphyritic, layered dark porphyritic, and cave dark porphyritic microfacies patterns; the massive facies pattern is subdivided into bright and dark massive microfacies patterns; the linear facies pattern is subdivided into regular linear and irregular linear microfacies patterns.

Through analysis of cores and thin sections, nine types of microfacies patterns represent different lithologies and sedimentary microfacies. The chaotic dark porphyritic microfacies pattern represents algal agglutinated dolomite, containing irregular dissolved pores formed by dissolution of algal agglutinate, which was deposited in the platform margin or intra-platform algal mound, being a shallow-water high-energy depositional environment. The layered dark porphyritic microfacies pattern represents algal detrital dolomite, containing intergranular pores and intragranular pores, which was deposited in the algal psammitic shoal at the platform margin, being a shallow-water high-energy depositional environment. The cave-filling microfacies pattern generally represents breccia dolomite, containing relatively large dissolved pores and caves, which was deposited in a high-energy depositional environment. The bright massive microfacies pattern represents siliceous algal laminae, which is tight non-reservoir formed in algal laminae mound under relatively weak hydrodynamic conditions. The dark massive microfacies pattern represents black dolomicrite, which is developed on the platform margin or between shoal and mound of restricted platform, being a relatively deepwater lowenergy depositional environment. The regular linear microfacies pattern represents black dolomicrite, with stylolite, which was deposited in low-energy tidal flat or shoal and mound. The irregular linear microfacies pattern represents algae-bearing psammitic dolomite, with microfracture network, which was formed in the psammitic shoal of platform margin. The layered facies pattern represents black dolomicrite, sometimes with siliceous strips, and the layer interface is often a set of nearly parallel high-conductivity anomalies with small and uniform width. The strip facies pattern represents a thin layer of fine crystal dolomite, formed in a lowenergy dolomite flat depositional environment.

4.3. Logging identification chart of microfacies

The microfacies identification by image log is a process that the geological data (e.g. core) are correlated with log data (e.g. image log) and finally a carbonate microfacies pattern chart is established. Firstly, sedimentary facies are divided depending on the image log based on core calibration, together with conventional logs. Then, the chart illustrating the correspondence between image log microfacies and microfacies is prepared. Finally, the microfacies are

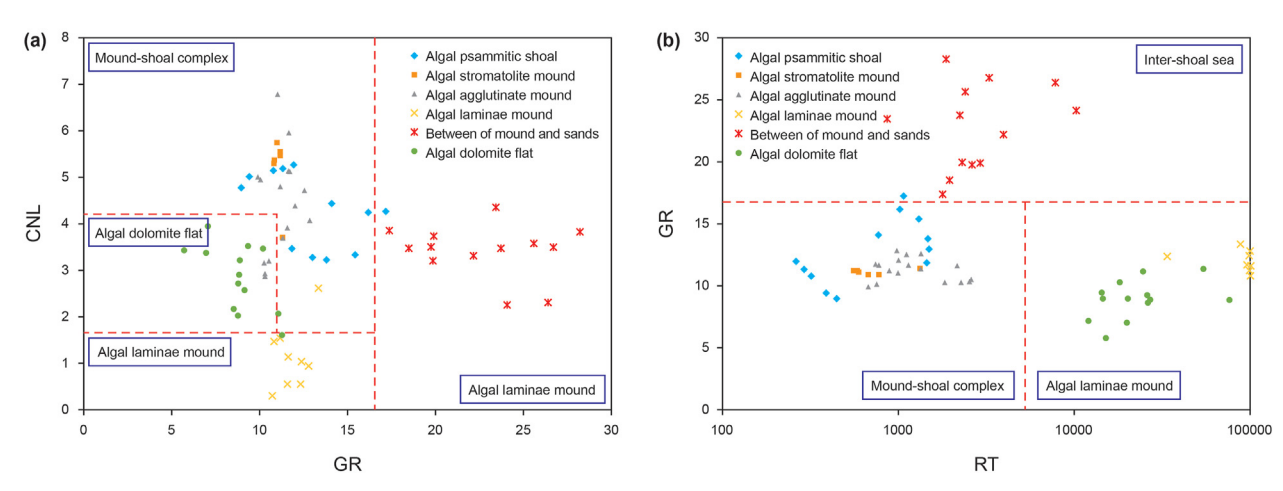


Fig. 3. a GR-CNL crossplot of platform margin microfacies. b GR-RT crossplot of platform margin microfacies.

Table 2Conventional logging identification criteria for carbonate microfacies of the Deng 4 Member in the Gaoshiti-Moxi area.

Microfacies	GR(API)	RT(ohm·m)	CNL (%)
Algal psammitic shoal (platform margin)	14–20	1000-4000	3.6-4.4
Algal laminae mound (platform margin)	14-22	>20000	0.2-2.8
Algal agglutinate mound (platform margin)	15-20	800-6000	2.8-5.1
Algal stromatolite mound (platform margin)	12-18	2000-6000	2.2-2.6
Dolomitic inter-shoal-mound (platform margin)	20-30	600-3000	2.4-4.4
Algal dolomite flat	7-20	>30000	0.1-2.8
Argillaceous dolomite flat	30-65	900-4000	1.7-2.7
Dolomite flat	10-20	6000-30000	0.6-2.7
Algal psammitic shoal (intra-platform)	10-20	200-3000	3.2-5.3
Algal agglutinate mound (intra-platform)	10-20	300-3000	3.2-5.4
Algal laminae mound (intra-platform)	10-15	>30000	0.3-2.6
Algal stromatolite mound (intra-platform)	10-15	300-2000	2.9-5.7
Dolomitic inter-shoal sea (intra-platform)	18-35	800-8000	2.6-3.6

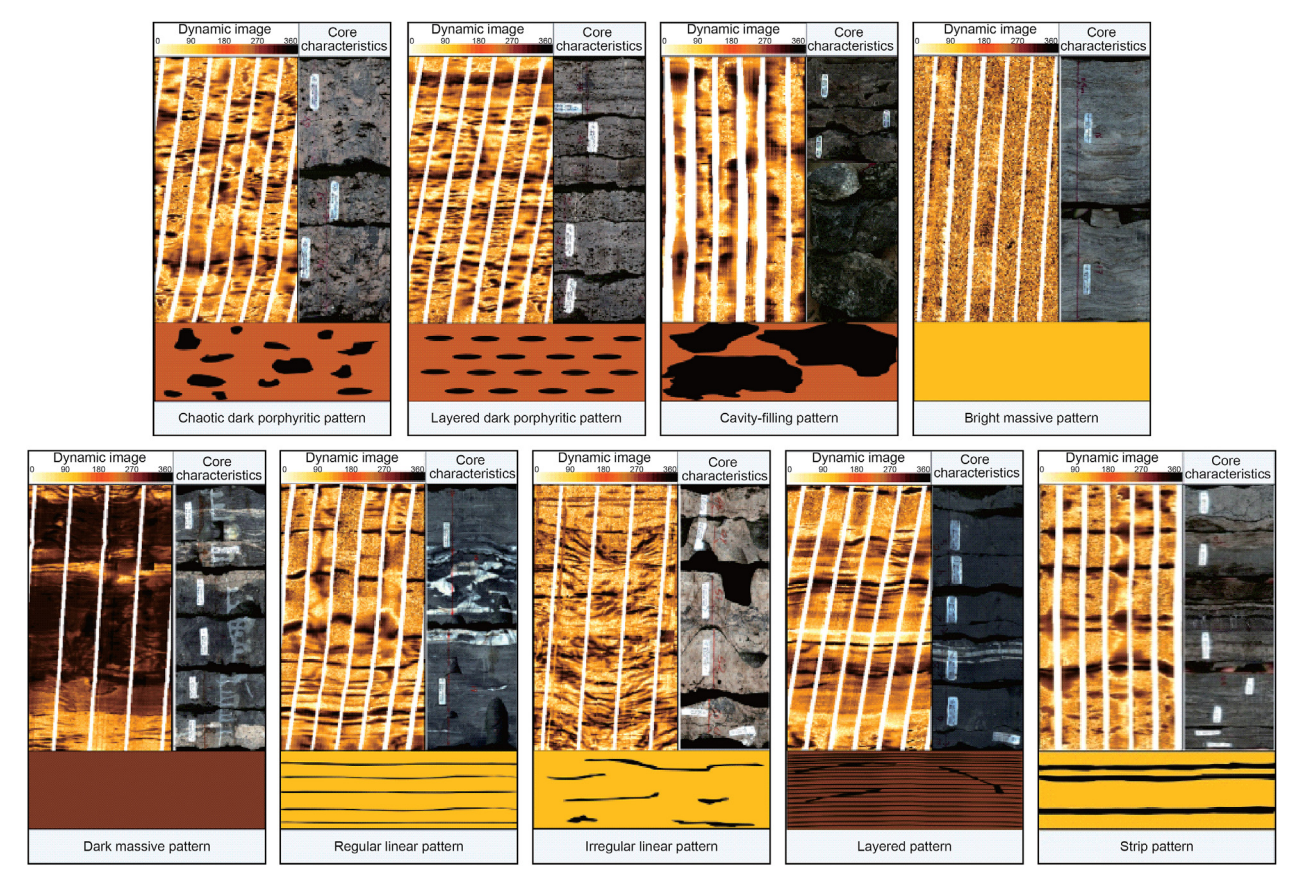


Fig. 4. Charts showing the image log facies/microfacies patterns of Deng 4 Member in the Gaoshiti-Moxi area.

identified via software or artificially. Based on the electrical image log responses, core restoration and facies description were made for 20 wells. Specifically, depth correlation was conducted between conventional GR log and imaging GR log, between core characteristics and image characteristics, and between conventional log porosity and core analysis porosity, thereby to achieve deep matching among conventional logs, image logs and core. Through clarifying the types of sedimentary facies in the coring interval, the microfacies are finely calibrated to their well logging response characteristics, so that the microfacies identification charts are prepared and the microfacies in non-coring interval are identified. Fig. 5 illustrates the typical microfacies identification charts and logging characteristics.

5. Discussion

According to the criteria for microfacies identification by conventional logs and image logs, a software module for automatic microfacies identification was developed on the CIFlog platform. With this software module, the full-borehole microfacies were divided for 60 wells in the Deng 4 Member of the Sichuan Basin. Fig. 6 shows the comprehensive evaluation column of sedimentary facies in Well A in the central Sichuan Basin. Moreover, according to the results of single-well microfacies division, multiple cross-well sections from the platform margin to intra-platform and inside platform margin and platform. Fig. 7 illustrates the variation of microfacies from the platform margin to the intra-platform, with

Q.-F. Feng, Y.-X. Xiao, X.-L. Hou et al. Petroleum Science 18 (2021) 1086-1096

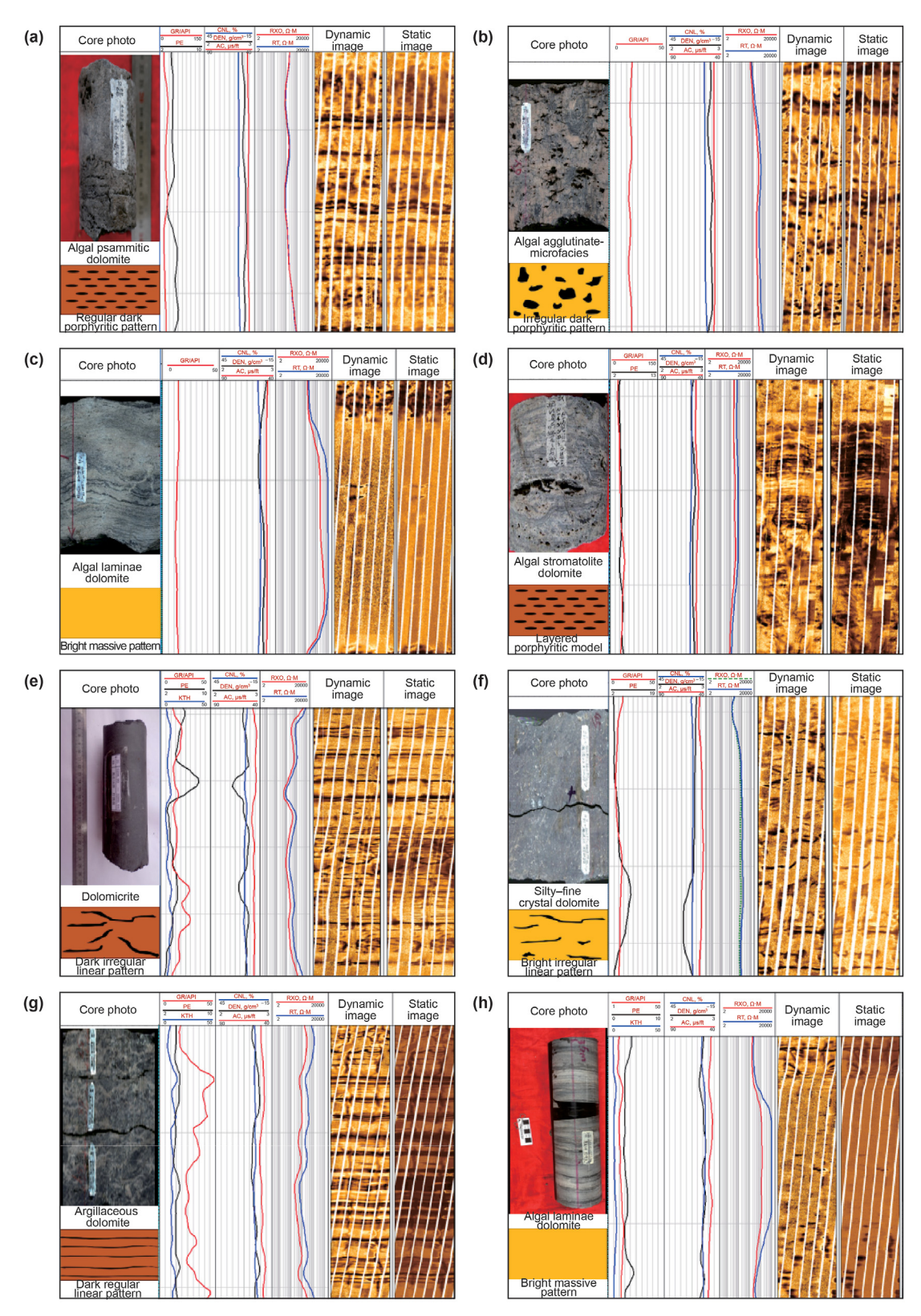


Fig. 5. a. Algal psammitic shoal microfacies, with low RT (200–3000 Ω m) and low GR (14–20APl) according to conventional logs, and showing regular dark porphyritic pattern (bedding-parallel or honeycomb) according to image log **b.** Algal agglutinate mound microfacies with low GR (9–20APl) and low RT (300–5000 Ω m) according to conventional logs, and showing irregular dark porphyritic pattern according to image log; **c.** Algal laminae mound microfacies, with low GR (13–21APl) and high RT (>20000 Ω m) according to conventional log, and showing bright massive pattern according to image logs; **d.** Algal stromatolite mound microfacies, with low GR (12–15APl) and low RT (2000–5000 Ω m) according to conventional log, and showing dark layered porphyritic pattern according to image logs; **e.** Dolomitic inter-shoal sea microfacies, with high GR (17–28APl) and low RT (800–8000 Ω m) according to conventional logs, and showing dark irregular linear pattern according to image log; **f.** Dolomite flat microfacies, with low GR (11–18APl) and high RT (6400–27000 Ω m) according to conventional logs, and showing bright linear pattern according to imaging logging. **g.** Argillaceous dolomite flat microfacies, with high GR (36–65APl) and low RT (900–4000 Ω m) according to conventional logsing, and showing dark regular linear or strip pattern according to imaging logging **h.** Algal dolomite flat microfacies, with low GR (7–18APl) and high RT (>30000 Ω m) according to conventional logs, and showing bright massive pattern according to image logs.

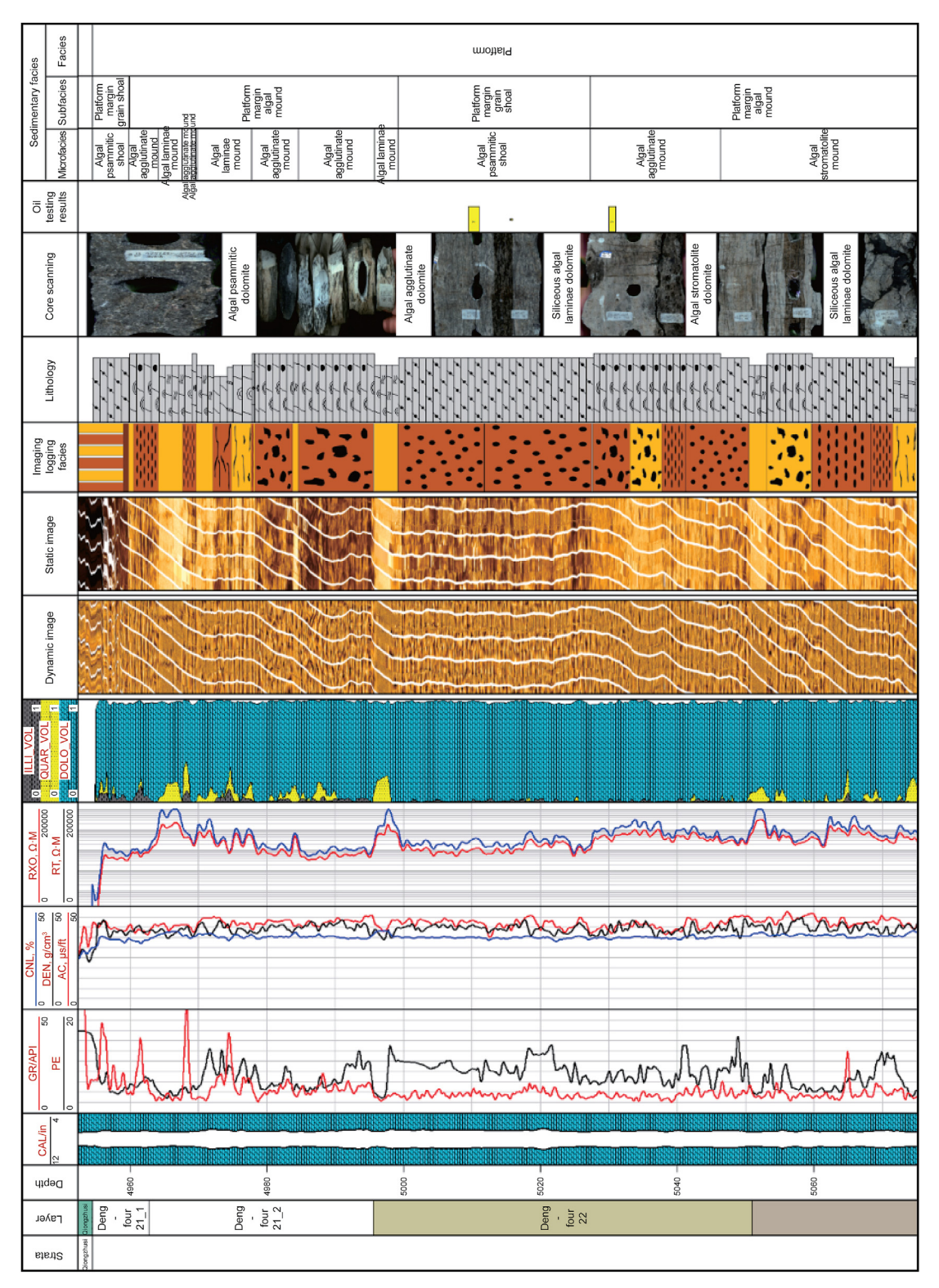


Fig. 6. Comprehensive evaluation column of single-well microfacies.

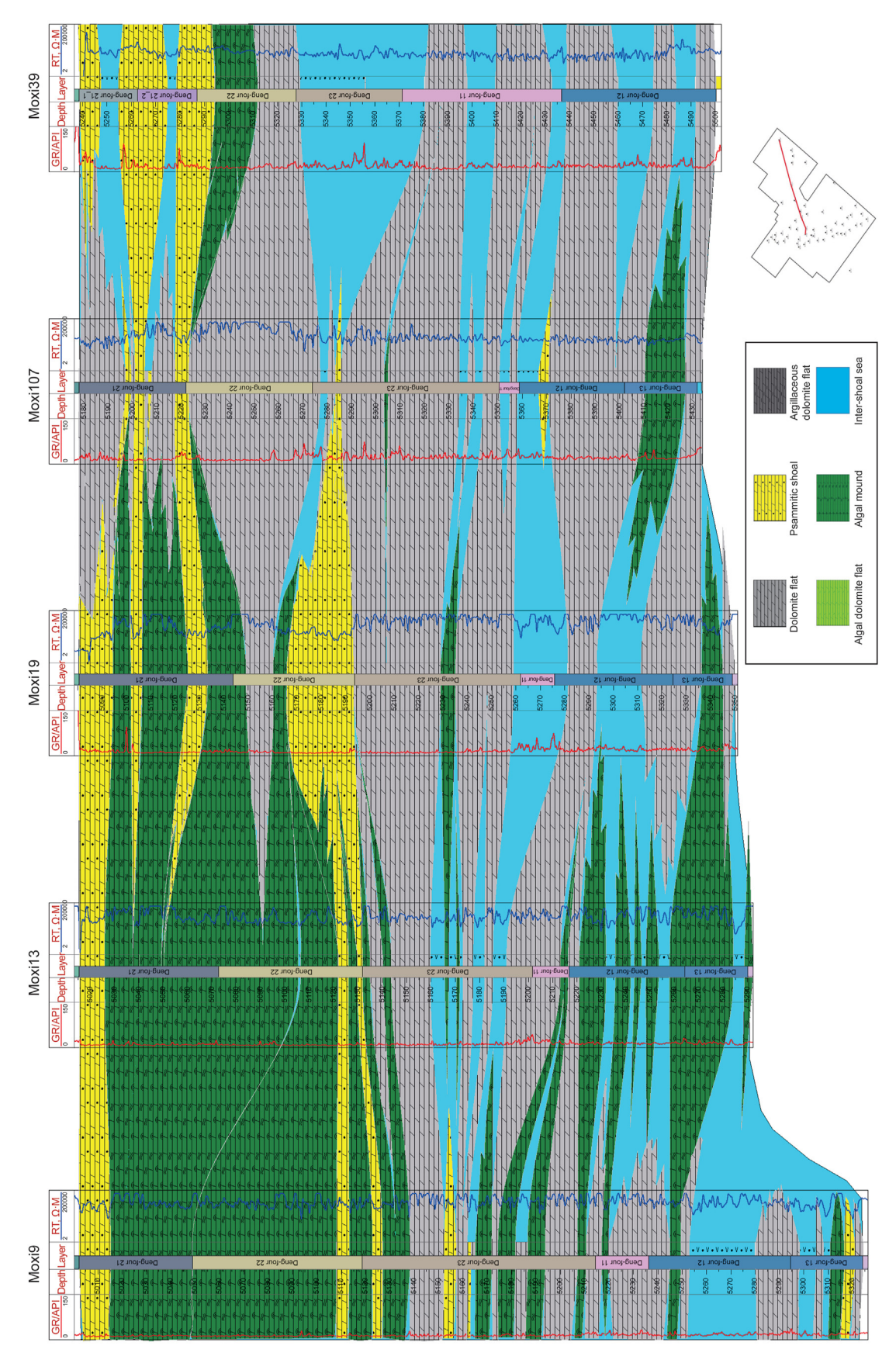


Fig. 7. Cross-well section of microfacies.

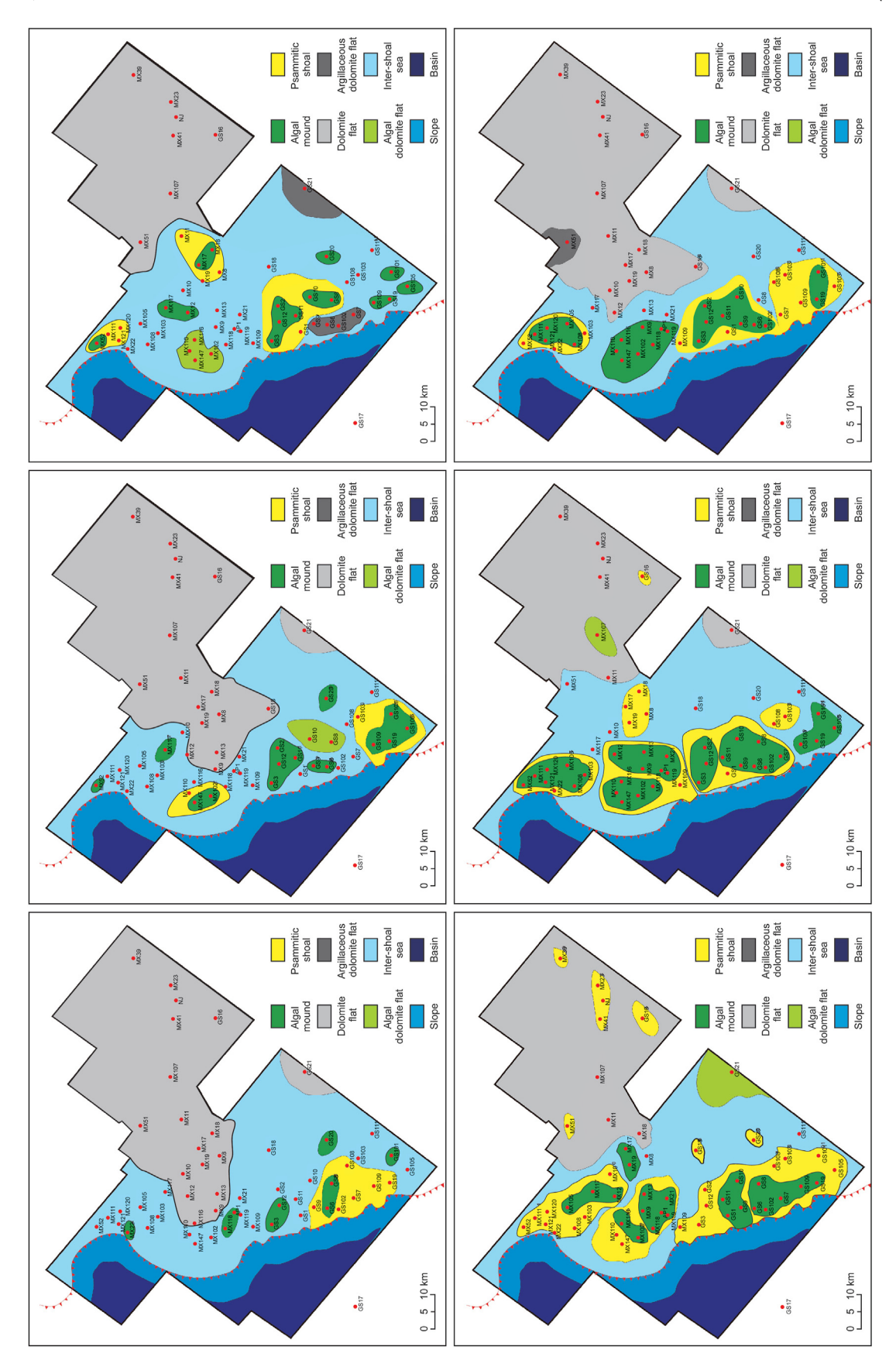


Fig. 8. Distribution of predicted microfacies in layers of Deng 4 Member in the Gaoshiti-Moxi area according to the logging evaluation.

Q.-F. Feng, Y.-X. Xiao, X.-L. Hou et al. Petroleum Science 18 (2021) 1086–1096

the psammitic shoal and algal mounds at the top and the dolomite flat microfacies at the bottom of the platform margin zone, and with decreasing psammitic shoal and algal mound at the top of intra-platform.

In the exploration and development practice, the Deng 4 Member is divided into upper and lower submembers, which are subdivided into six layers: Deng4²¹, Deng4²², Deng4²³, Deng4¹¹, Deng4¹², and Deng 4¹³, from top to bottom. Combined with the vertical division of microfacies for 60 exploratory wells in the Gaoshiti-Moxi area, the inter-well interpolation technique was used to prepare the plane map of predicted microfacies distribution for each layer (Fig. 8). It can be seen that, in the upper Deng 4 Member, the mound-shoal complexes are contiguous at the platform margin, and the reservoirs are continuous. Especially in Deng4²³ at the top of the Deng 4 Member, the mound-shoal complexes cover a wider range, while the inter-shoal sea is shrunk. This position is most favorable for exploration and development.

Inside the platform, in the upper Deng 4 Member, dolomite flat is dominant, and argillaceous dolomite flat is observed locally. In Deng4²², the dolomite flat coverage becomes smaller, and grain shoal appears. In Deng4²¹, grain shoal expands further. In the lower Deng 4 Member, the platform margin mound-shoal complex is sporadically developed, the reservoir is less continuous, inter-shoal sea is widespread, and algal dolomite flat and argillaceous dolomite flat are developed locally. However, a largescale of mound-shoal complex is observed in Well Gaoshi1in Deng4¹³, and also in Well Gaoshi 109 in Deng4¹². However, dolomite flat and inter-shoal sea dominate the lower Deng4 Member across the platform, while mound-shoal complex is only found locally in Deng4¹³.

6. Conclusions

The Deng 4 Member in the Gaoshiti-Moxi area can be divided into 2 facies: platform margin and restricted platform. The platform margin facies are subdivided into 3 subfacies: platform margin algal mound, platform margin grain shoal, and inter-shoal sea. The restricted platform facies are subdivided into 4 subfacies: intraplatform grain shoal, intra-platform algal mound, platform flat, and inter-shoal sea.

A method combining conventional logs and high-resolution electrical image logs is proposed to identify the sedimentary microfacies. The crossplots of GR, CNL and RT can effectively distinguish the microfacies of algal laminae mound, inter-shoal sea, and mound-shoal complex. Totally, 9 types of image log microfacies patterns were established; coupling with the conventional well logging response characteristics, 8 types of "core + conventional log + image log" microfacies identification charts were formed. The platform margin is characterized by the superposition of platform margin algal mounds and platform margin shoals.

The mound-shoal complex is better developed in the upper Deng 4 Member than the lower Deng 4 Member, and in the platform margin than the intra-platform. Upwardly, the mound-shoal complex becomes broader — transiting from sporadic distribution to continuous distribution, and the continuity of reservoir becomes better. Inside the platform, dolomite flat and inter-shoal sea is dominant in the lower Deng 4 Member, and intra-platform mound-shoal complex is developed at the top of the upper Deng 4 Member. The proposed facies/microfacies identification method is very applicable and can be extended to the identification of marine carbonate microfacies in other strata.

Acknowledgements

This work is financially supported by oil and gas accumulation patterns, key technologies and targets evaluation of Lower Paleozoic-Precambrian carbonate rocks (No.2016ZX05004). We thank the PetroChina Xinan Oilfield Company for their assistance in providing the information, and for their technical input to this work. We thank the staff of China University of Petroleum, Beijing. Professor Guiwen Wang and Dr. Jin Lai are acknowledged for providing technology help. The authors also thank associate editor of Petroleum Science for his enthusiasm, patience, and tireless efforts

References

- Li, P.W., Jin, T.F., Wang, G.Q., et al., 2013. Microbial carbonates and their significance in the petroleum exploration. Geol. Sci. Technol. Inf. 32 (3), 66–74. https://doi.org/10.1144/SP418.14, 1000-7849(2013)32:3<66:WSWTSY>2.0.TX;2-1. (in Chinese).
- Awdal, A., Healy, D., Alsop, G.I., 2016. Fracture patterns and petrophysical properties of carbonates undergoing regional folding: a case study from Kurdistan, N Iraq. Mar. Petrol. Geol. 71, 149–167. https://doi.org/10.1016/j.marpetgeo.2015.12.017.
- Brekke, H., MacEachern, J.A., Roenitz, T., et al., 2017. The use of microresistivity image logs for facies interpretations: an example in point-bar deposits of the McMurray Formation, Alberta, Canada. AAPG (Am. Assoc. Pet. Geol.) Bull. 101 (5), 655–682. https://doi.org/10.1306/08241616014.
- Duan, J.B., Dai, L.C., Li, B.S., et al., 2019. Reservoir characteristics and their controlling factors of the fourth member of upper sinian dengying Fm in the northern Sichuan Basin. Nat. Gas. Ind. 39 (7), 7–20. https://doi.org/10.1016/S1876-3804(20)60127-1, 1000-0976(2019)39:7<9:SCPDBB>2.0.TX;2-T. (in Chinese).
- Folkestad, A., Veselovsky, Z., Roberts, P., 2012. Utilising borehole image logs to interpret delta to estuarine system: a case study of the subsurface lower Jurassic Cook formation in the Norwegian northern North Sea. Mar. Petrol. Geol. 29 (1), 255–275. https://doi.org/10.1016/j.marpetgeo.2011.07.008.
- Geng, H.J., Wang, G.W., Li, J., et al., 2002. Image interpretation modes and the typical interpretation chart for Imaging Well logging. Journal of Jianghan Petroleum Institute 24 (1), 26–29, 1000-9752(2002)24:1<26:CXCJTX>2.0.TX;2-M. (in Chinese).
- Goodall, T.M., Moller, N.K., Ronningsland, T.M., 1998. The integration of electrical image logs with core data for improved sedimentological interpretation. Geological Society, London, Special Publications 136 (1), 237–248. https:// doi.org/10.1144/GSL.SP.1998.136.01.20.
- Hollis, C., Vahrenkamp, V., Tull, S., et al., 2010. Pore system characterisation in heterogeneous carbonates: an alternative approach to widely-used rock-typing methodologies. Mar. Petrol. Geol. 27 (4), 772–793. https://doi.org/10.1016/ j.marpetgeo.2009.12.002.
- Hu, M.Y., Gao, D., Wei, G.Q., et al., 2019. Sequence stratigraphy and facies architecture of a mound-shoal-dominated dolomite reservoir in the late Ediacaran Dengying Formation, central Sichuan Basin, SW China. Geol. J. 54 (3), 1653–1671. https://doi.org/10.1002/gj.3261.
- Keeton, G.I., Pranter, M.J., Cole, R.D., et al., 2015. Stratigraphic architecture of fluvial deposits from borehole images, spectral-gamma-ray response, and outcrop analogs, Piceance Basin, Colorado. AAPG (Am. Assoc. Pet. Geol.) Bull. 99 (10), 1929–1956. https://doi.org/10.1306/05071514025.
- Khoshbakht, F., Memarian, H., Mohammadnia, M., 2009. Comparison of Asmari, Pabdeh and Gurpi formation's fractures, derived from image log. J. Petrol. Sci. Eng. 67 (1–2), 65–74. https://doi.org/10.1016/j.petrol.2009.02.011.
- Khoshbakht, F., Azizzadeh, M., Memarian, H., et al., 2012. Comparison of electrical image log with core in a fractured carbonate reservoir. J. Petrol. Sci. Eng. 86–87, 289–296. https://doi.org/10.1016/j.petrol.2012.03.007.
- Lai, J., Wang, G.W., Fan, Z.Y., et al., 2017. Sedimentary characterization of a braided delta using well logs: the Upper Triassic Xujiahe formation in central Sichuan basin, China. J. Petrol. Sci. Eng. 154, 172–193. https://doi.org/10.1016/ i.petrol.2017.04.028.
- Lai, J., Wang, G.W., Wang, S., et al., 2018. A review on the applications of image logs in structural analysis and sedimentary characterization. Mar. Petrol. Geol. 95, 139–166. https://doi.org/10.1016/j.marpetgeo.2018.04.020.
- Lai, J., Pang, X., Xiao, Q., et al., 2019. Prediction of reservoir quality in carbonates via porosity spectrum from image logs. J. Petrol. Sci. Eng. 173, 197–208. https:// doi.org/10.1016/j.petrol.2018.10.022.
- Lai, J., Wang, S., Zhang, C.S., et al., 2020. Spectrum of pore types and networks in the deep cambrian to lower ordovician dolostones in tarim basin, China. Mar. Petrol. Geol. 112, 104081. https://doi.org/10.1016/j.marpetgeo.2019.104081.
- Lan, C.J., Xu, Z.H., Ma, X.L., et al., 2019. Development and distribution of mound-shoal complex in the sinian Dengying Formation, Sichuan Basin and its control on reservoirs. Acta Pet. Sin. 40 (9), 1069–1084. https://doi.org/10.1016/51876-3804(13)60096-8, 0253-2697(2019)40:9<1069:SCPDZD>2.0.TX;2-N. (in Chinese).
- Li, L., Tan, X.C., Zeng, W., et al., 2013. Development and reservoir significance of mud mounds in sinian Dengying Formation, Sichuan Basin. Petrol. Explor. Dev. 40 (6), 714–721. https://doi.org/10.1016/S1876-3804(13)60096-8.
- Li, N., Xiao, C.W., Wu, L.H., et al., 2014. The innovation and development of log evaluation for complex carbonate reservoir in China. Journal of Well Logging Technology 38 (1), 1–10. https://doi.org/10.1016/j.ngib.2016.03.004, 1004-1338(2014)38:1<1:FZTSYY>2.0.TX;2-B. (in Chinese).

- Liu, S.G., Song, J.M., Luo, P., et al., 2016. Characteristics of microbial carbonate reservoir and its hydrocarbon exploring outlook in the Sichuan Basin, China. J. Chengdu Univ. Technol. (Sci. Technol. Ed.) 43 (2), 129–152, 1671–9727(2016) 43:2<129:SCPDSC>2.0.TX;2-H. (in Chinese).
- Luo, B.W., Jia, C.Z., Wei, G.Q., 2015. Characteristics and models of weathering paleokarst in upper sinian, Sichuan Basin. Journal of China University of Petroleum 39 (3), 8–19. https://doi.org/10.1016/j.ptlrs.2017.06.003, 1673-5005(2015)39: 3<8:SCPDSZ>2.0.TX;2-D, (in Chinese).
- Luo, W.J., Xu, W., Zhu, Z.P., et al., 2019. Origin of siliceous rocks in sinian dengying 4 member, Gaoshiti area, Sichuan Basin. Natural Gas Exploration and Development 42 (3), 1–9. https://doi.org/10.12055/gaskk.issn.1673-3177.2019.03.001 (in Chinese).
- Mancini, E.Á., Benson, D.J., Hart, B.S., et al., 2000. Appleton field case study (eastern Gulf coastal plain): field development model for Upper Jurassic microbial reef reservoirs associated with paleotopographic basement structures. AAPG (Am. Assoc. Pet. Geol.) Bull. 84 (11), 1699–1717. https://doi.org/10.1306/8626C36B-173B-11D7-8645000102C1865D.
- Mancini, E.A., Parcell, W.C., Ahr, W.M., et al., 2008. Upper Jurassic updip stratigraphic trap and associated Smackover microbial and nearshore carbonate facies, Eastern Gulf Coastal Plain. AAPG (Am. Assoc. Pet. Geol.) Bull. 92 (4), 417–442. https://doi.org/10.1306/11140707076.
- Norbisrath, J.H.G.P., Eberli, B., Laurich, G., et al., 2015. Urai. Electrical and fluid flow properties of carbonate microporosity types from multiscale digital image analysis and mercury injection. AAPG (Am. Assoc. Pet. Geol.) Bull. 99 (11), 2077–2098. https://doi.org/10.1306/07061514205.
- Riding, R., 1991. Calcareous Algae and Stromatolites. Springer-Verlag, Berlin, pp. 21–51.
- Riding, R., 2000. Microbial carbonates: the geological record of calcified bacterialalgal mats and biofilms. Sedimentology 47 (Suppl. 1), 179–214. https:// doi.org/10.1046/j.1365-3091.2000.00003.x.
- Roth, S., Biswal, B., Afshar, G., et al., 2011. Continuum-based rock model of a reservoir dolostone with four orders of magnitude in pore sizes. AAPG (Am. Assoc. Pet. Geol.) Bull. 95 (6), 925–940. https://doi.org/10.1306/12031010092.
- Shan, X.Q., Zhang, J., Zhang, B.M., et al., 2016. Dolomite karst reservoir characteristics and dissolution evidences of sinian Dengying Formation, Sichuan Basin. Acta Pet. Sin. 37 (1), 17–29. https://doi.org/10.7623/syxb201601002 (in Chinese).
- Song, J.M., Liu, S.G., Sun, W., et al., 2013. Control of xingkaitaphrogenesis on Dengying Formation high quality reservoirs in upper sinian of Sichuan Basin. J. Chengdu Univ. Technol. (Sci. Technol. Ed.) 40 (6), 658–670. https://doi.org/10.3969/j.issn.1671-9727.2013.06.04 (in Chinese).
- Song, J.M., Liu, S.G., Li, Z.W., et al., 2017. Characteristics and controlling factors of microbial carbonate reservoirs in the upper sinian Dengying Formation in the Sichuan Basin. Oil Gas Geol. 38 (4), 741–752. https://doi.org/10.11743/ogg20170411 (in Chinese).
- Wang, W.Z., Yang, Y.M., Wen, L., et al., 2016. A study of sedimentary characteristics of microbial carbonate: a case study of the Sinian Dengying Formation in Gaoshiti-Moxi area, Sichuan Basin. Chin. Geol. 43 (1), 306—318. https://doi.org/10.12029/gc20160123 (in Chinese).
- Wang, Z.C., Liu, J.J., Jiang, H., et al., 2019. Lithofacies paleogeography and exploration significance of Sinian Doushantuo depositional stage in the middle-upper

- Yangtze region, Sichuan Basin, SW China. Petrol. Explor. Dev. 46 (1), 41–53. https://doi.org/10.1016/S1876-3804(19)30004-7.
- Wang, G.W., Lai, J., Liu, B.C., et al., 2020. Fluid property discrimination in dolostone reservoirs using well logs. Acta Geol. Sin. 94 (3), 831–846. https://doi.org/ 10.1111/1755-6724.14526.
- Wei, G.Q., Du, J.H., Xu, C.C., et al., 2015a. Characteristics and accumulation modes of large gas reservoirs in Sinian-Cambrian of Gaoshiti-Moxi region, Sichuan Basin. Acta Pet. Sin. 36 (1), 1–12. https://doi.org/10.1016/S2096-2495(17)30040-6, 0253-2697(2015)36:1<1:SCPDGS>2.0.TX;2-A. (in Chinese).
- Wei, G.Q., Xie, Z.Y., Song, J.R., et al., 2015b. Features and origin of natural gas in the Sinian-Cambrian of central Sichuan paleo-uplift, Sichuan Basin, SW China. Petrol. Explor. Dev. 42 (6), 768–777. https://doi.org/10.1016/S1876-3804(15) 30073-2
- Wen, L., Wang, W.Z., Zhang, J., et al., 2017. Classification of sinian Dengying Formation and sedimentary evolution mechanism of gaoshiti-moxi area in central Sichuan Basin. Acta Petrol. Sin. 33 (4), 1285—1294. https://doi.org/10.1016/S1876-3804(20)60127-1, 1000-0569(2017)33:4<1285:CZGSTM>2.0.TX;2-B. (in Chinese).
- Westphal, H., Surholt, I., Kiesl, C., et al., 2005. NMR measurements in carbonate rocks: problems and an approach to a solution. Pure Appl. Geophys. 162 (3), 549–570. https://doi.org/10.1007/s00024-004-2621-3.
- Wu, Y.Y., Zhang, W.M., Tian, C.B., et al., 2013. Application of Image logging in identifying lithologies and semimetal facies in Reef-Shoal Carbonate reservoirtake Rumaila oil field in Iraq for example. Prog. Geophys. 28 (3), 1497–1506. https://doi.org/10.6038/pg20130345 (in Chinese).
- Xu, C., Cronin, T.P., McGinness, T.E., et al., 2009. Middle Atokan sediment gravity flows in the Red Oak field, Arkoma Basin, Oklahoma: a sedimentary analysis using electrical borehole images and wireline logs. AAPG (Am. Assoc. Pet. Geol.) Bull. 93 (1), 1–29. https://doi.org/10.1306/09030808054.
- Yang, W., Wei, G.Q., Zhao, R.R., et al., 2014. Characteristics and distribution of karst reservoirs in the sinian dengying Fm, Sichuan Basin. Journal of Gas Industry 34 (3), 55–60. https://doi.org/10.3787/j.issn.1000-0976.2014.03.009 (in Chinese).
- Yang, Y., Huang, X.P., Zhang, J., et al., 2014. Characteristics and geologic significances of the top Sinian karst landform before the Cambrian deposition in the Sichuan Basin. Journal of Gas Industry 34 (3), 38–43. https://doi.org/10.3787/j.issn.1000-0976.2014.03.0016 (in Chinese).
- Yao, G.S., Hao, Y., Zhou, J.G., et al., 2014. Formation and evolution of reservoir spaces in the sinian dengying Fm of Sichuan Basin. Journal of Gas Industry 34 (3), 34–37, 0.3787/j.issn.1000-0976.2014.03.005. (in Chinese)
- Zhang, X.H., Peng, H.L., Tian, X.W., et al., 2019. Influence of difference among biohermshoal facies reservoirs on exploration model: an example from Sinian Dengying Formation, central Sichuan Basin. Natural Gas Exploration and Development 42 (2), 13–21, 0.12055/gaskk.issn.1673-3177.2019.02.002. (in Chinese).
- Zhou, J.G., Zhang, J.Y., Deng, H.Y., et al., 2017. Lithofacies paleogeography and sedimentary model of sinian dengying Fm in the Sichuan Basin. Journal of Gas Industry 37 (1), 24–31, 0.3787/j.issn.1000-0976.2017.01.003. (in Chinese).
- Zou, C.N., Du, J.H., Chun, C.C., et al., 2014. Formation, distribution, resource potential and discovery of the Sinian—Cambrian giant gas field, Sichuan Basin, SW China. Petrol. Explor. Dev. 41 (3), 278—293. https://doi.org/10.11698/PED.2014.03.03 (in Chinese).